Formulation of carbon black-ionomer dispersions for thin film formation in fuel cells

Eva Hoffmann, Su Zhang, Martin Thoma, Cornelia Damm, Wolfgang Peukert*

Supplementary materials

Supplementary material 1. Structure analysis of carbon black types

To observe the different carbon black structures visually, suspensions with an $I/C = 0$ (Composition 1, Table 1) were highly diluted (0.04 wt% carbon black) in a 87 wt% diacetone alcohol (DAA) in water mixture, treated with ultrasound for 30 min, spread on a silicon wafer and dried at ambient conditions. Afterwards the carbon aggregate/agglomerate structure was evaluated via SEM micrographs (see images below). Large carbon black agglomerates as well as smaller aggregate structures are visible. It seems that the tendency to form large agglomerates is more pronounced for the CB2 suspension, as the CB1 suspension shows smaller carbon clusters.

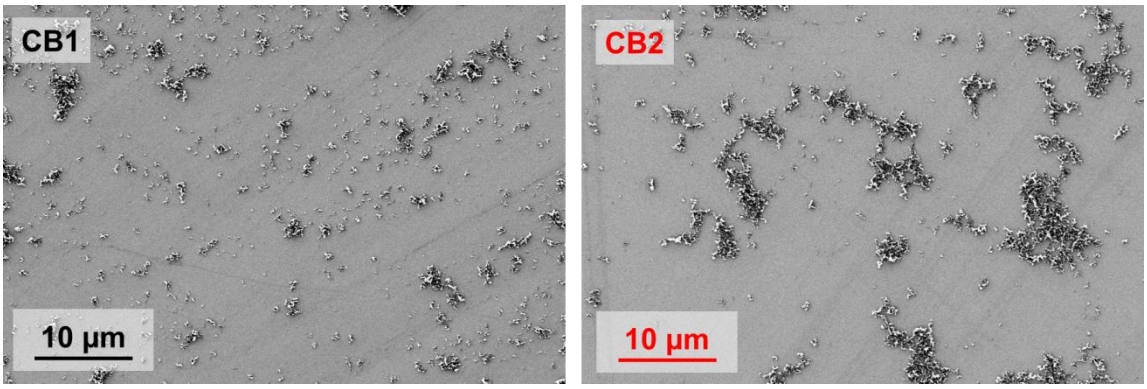

SEM images of diluted suspensions of CB1 (left) and CB2 (right) in an DAA/water mixture without addition of ionomer ($I/C = 0$)

By image analysis of the eight single SEM images with 2000x magnification (grey scale evaluation), cumulative number distributions of the particle size as well as form factor distributions for both suspensions could be obtained.

The area equivalent particle diameter x_{area} in µm was determined with A being the projection area in µm² of a carbon black particle.

$$x_{\text{area}} = \sqrt{\frac{A}{}}$$

Assuming ideal sphere geometry of the particles, with x_{area} the particle volume V_{p} can be calculated and therewith cumulative volume distributions are created.

$$V_{\text{p}} = \frac{1}{6}\ x_{\text{area}}^3$$

One can observe smaller particles for the CB1 (Figure below, left).

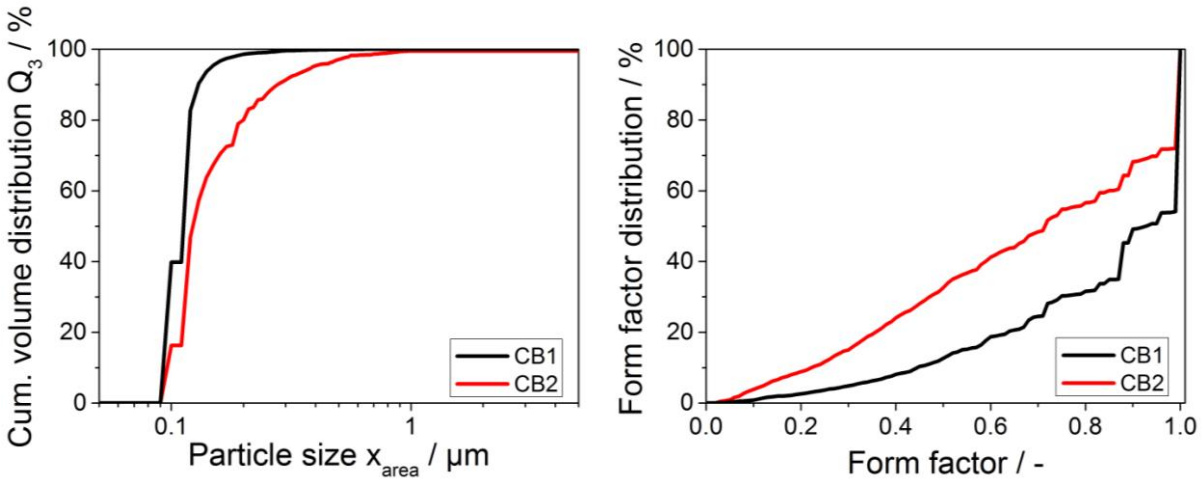

Particle size distribution (left) and form factor distribution (right) of highly diluted ultrasound-treated suspensions (0.04 wt% carbon black in a 87 wt% DAA in water mixture) without ionomer ($I/C = 0$) determined by image analysis of SEM micrographs.

The form factor is calculated according to the following equation with the projection area A in µm² and the circumference C of the particle in µm. An ideal circle exhibits a form factor of 1. The more the particle shape diverges from an ideal circle, the smaller the form factor.

$$form\ factor = 4\ \frac{A}{C^2}$$

Figure above, right, shows the form factor distributions of the two diluted suspensions. One can clearly see, that the CB2 suspension exhibits smaller form factors, indicating a more fractal structure of the carbon black aggregates.

Additionally transmission electron (TEM) images were taken of both carbon blacks (suspended in Ethanol, treated with Ultrasound and spread on a TEM copper grid) but structural differences in terms of aggregate and agglomerate structure are not evident here, as images are too detailed.

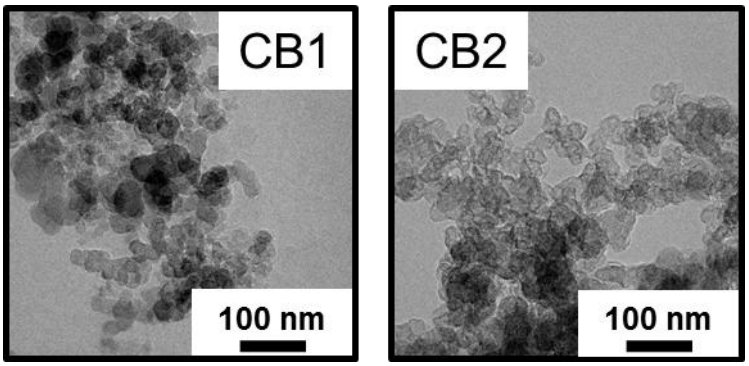

Supplementary material 2. XRD diffractograms of CB1 and CB2

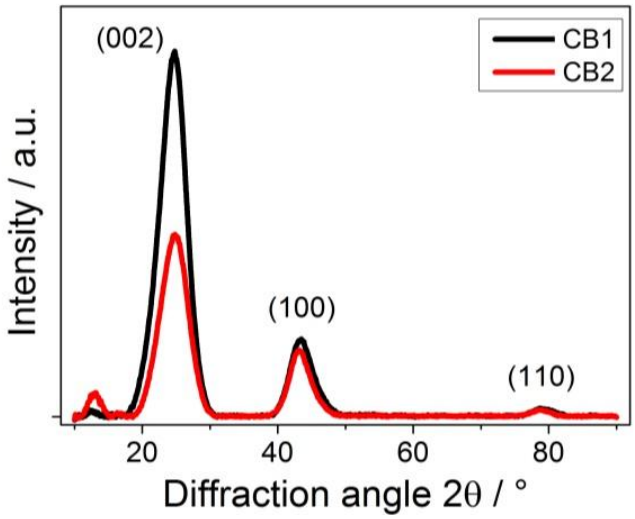

Supplementary material 3. Raman spectra of CB1 and CB2

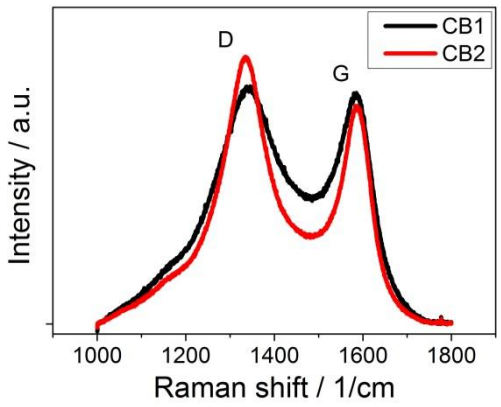

Supplementary material 4. Viscosity of CB1 suspensions as a function of *I/C* ratio for different shear rates

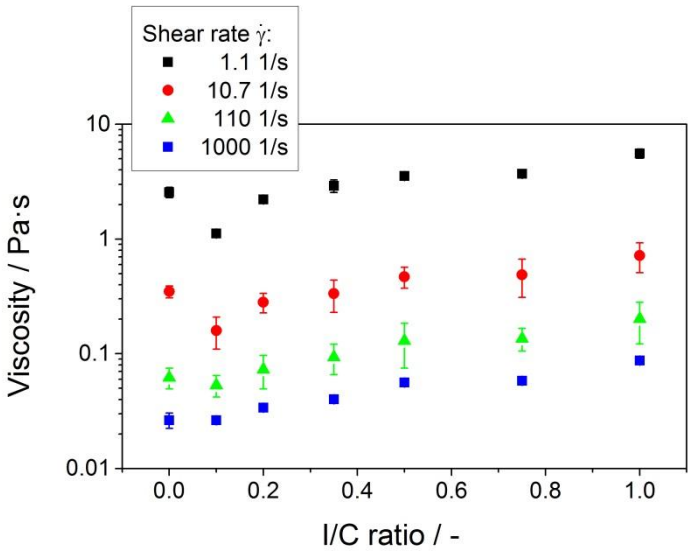

Supplementary material 5. Mathematical derivation of linear Ostwald/de Waele fitting curve

Power law: $\tau = \kappa\dot{\gamma}^n$

Viscosity function: $\tau = \dot{\gamma}\,\eta$

→ $\dot{\gamma}\,\eta = \kappa\dot{\gamma}^n$

→ $\eta = \kappa\dot{\gamma}^{n-1}$

Logarithm: $\log(\eta) = \log(\kappa\dot{\gamma}^{n-1})$

$\log(\eta) = \log(\kappa) + \log(\dot{\gamma}^{n-1})$

→ $\log(\eta) = \log(\kappa) + (n-1)\log(\dot{\gamma})$

Supplementary material 6. Ostwald/de Waele fitting for CB1

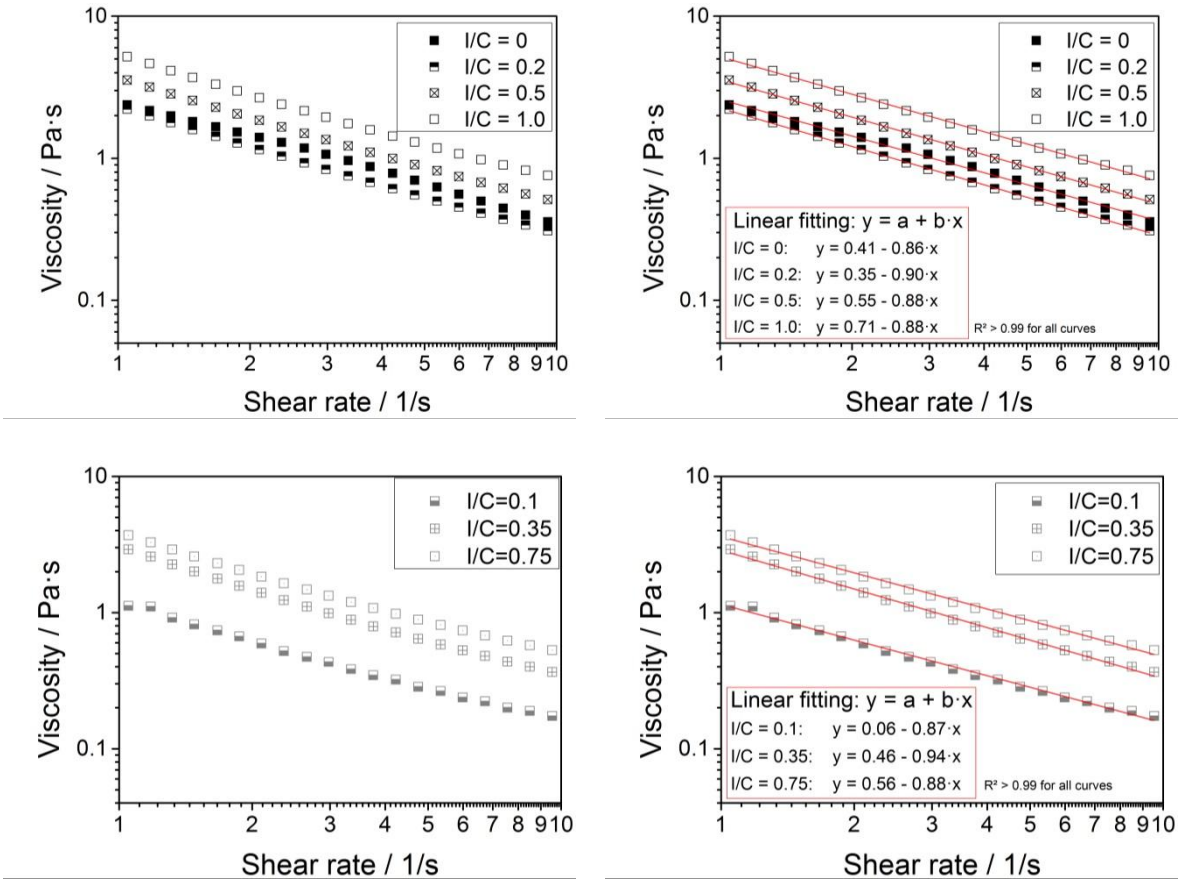

Supplementary material 7. Ostwald/de Waele fitting for CB2

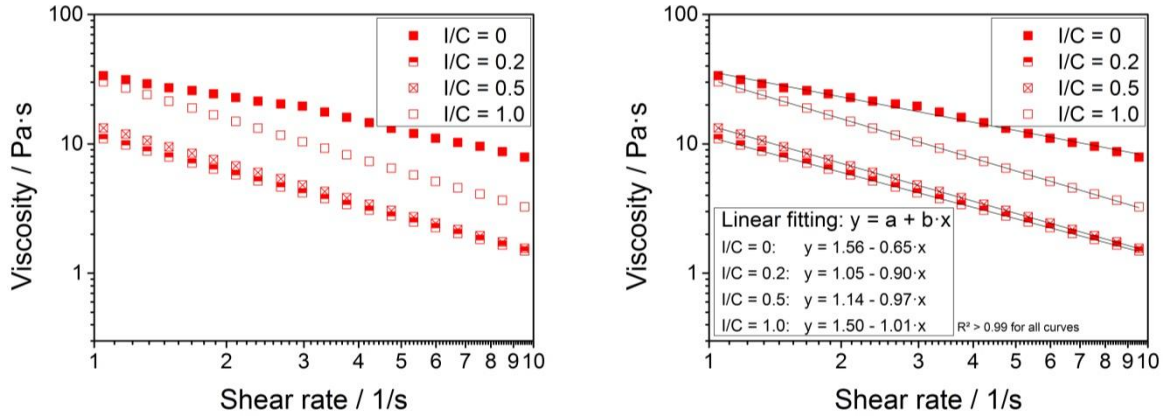

Supplementary material 8. Amplitude sweep of CB1 suspensions with varying *I/C* ratio

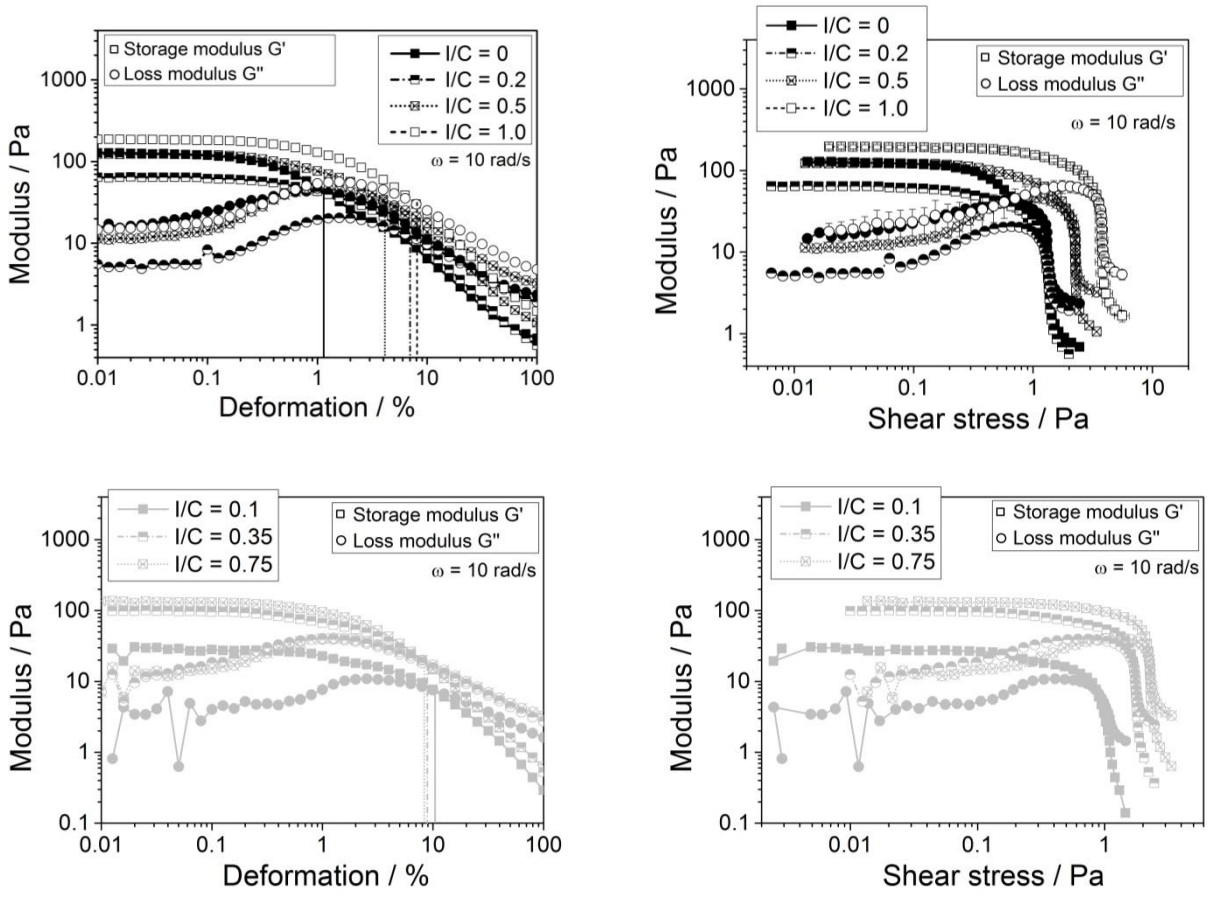

Supplementary material 9. Amplitude sweep of CB2 suspensions with varying *I/C* ratio

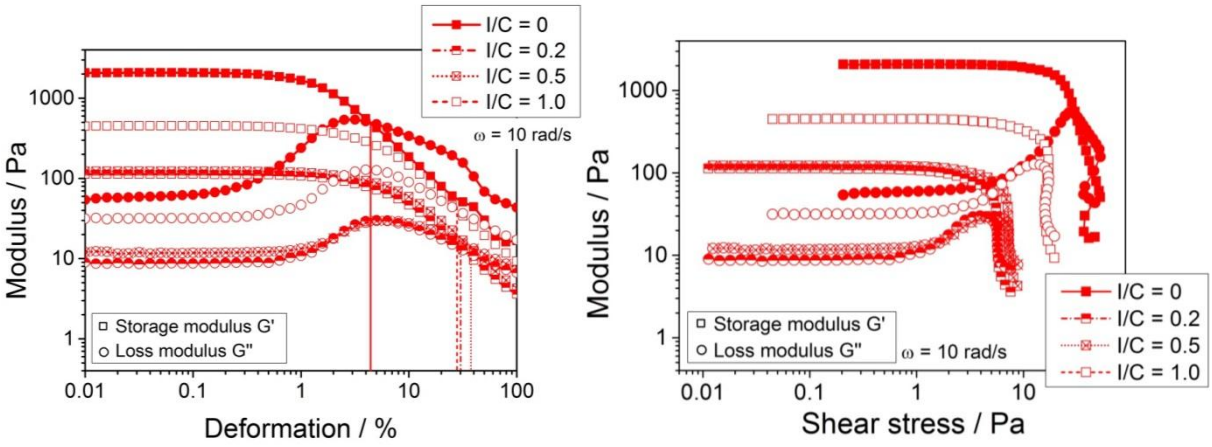

Supplementary material 10. Integral transmission curves of analytical centrifugation experiments of CB1 and CB2 suspensions with *I*/*C* ratio of 0 and 1 without (left) and with fitting curves (right); upper row: whole sedimentation run, lower row: sedimentation till 10000 s

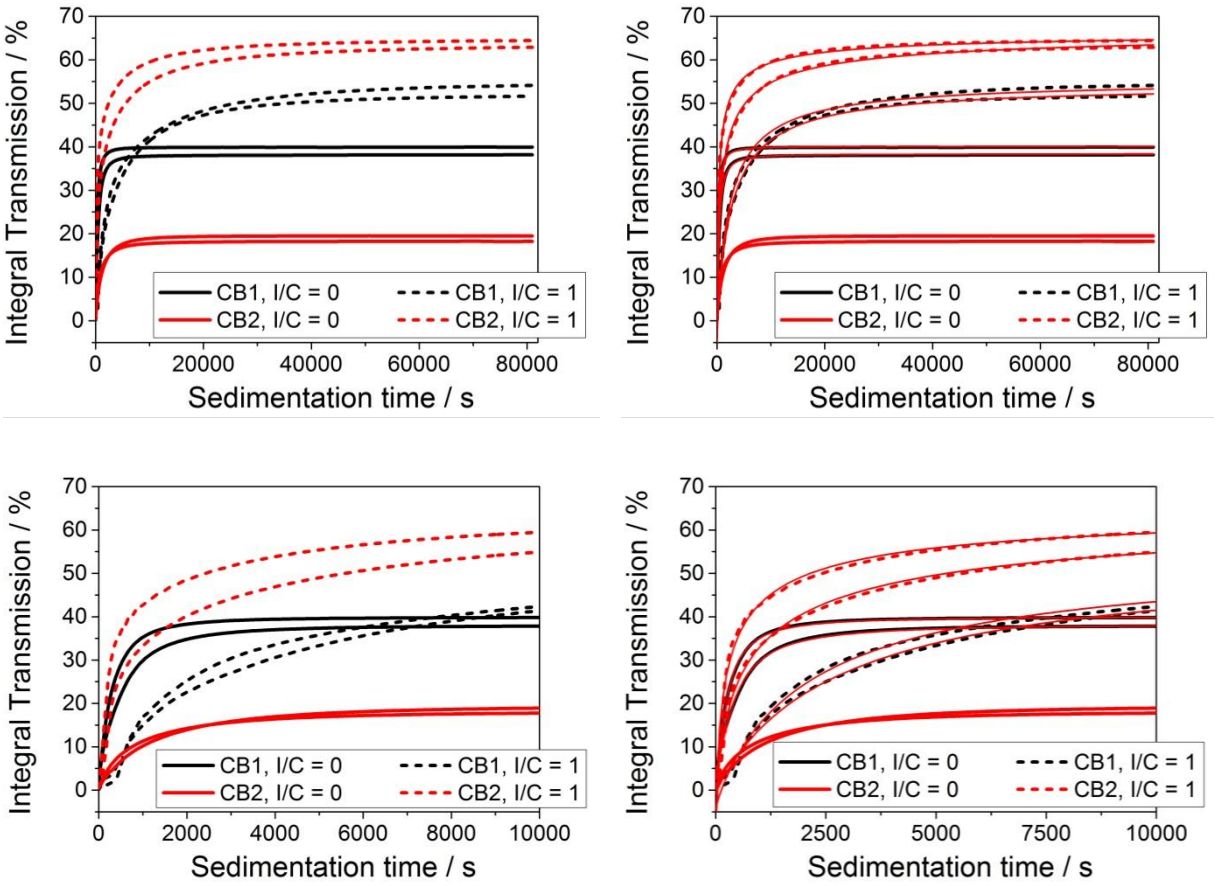

Supplementary material 11. Summary of sedimentation analysis parameters for CB1 and CB2 suspensions with varying ionomer content

1	$T_{end}/2$ (%)	t_{50} (s)	*RST* (10^7 s²/m²)
CB1, *I*/*C* = 0	19.6	306	5.5
CB1, *I*/*C* = 0.1	10.0	160510	2042.6
CB1, *I*/*C* = 0.2	19.3	4662	46.0
CB1, *I*/*C* = 0.35	16.2	1473	12.3
CB1, *I*/*C* = 0.5	31.8	816	5.8
CB1, *I*/*C* = 0.75	26.4	2530	13.3
CB1, *I*/*C* = 1.0	27.5	2762	11.1
CB2, *I*/*C* = 0	9.6	788	14.1
CB2, *I*/*C* = 0.2	16.1	4949	47.4
CB2, *I*/*C* = 0.5	19.6	3732	26.1
CB2, *I*/*C* = 1.0	33.6	747	3.0

Supplementary material 12. Filled cuvettes after end of sedimentation run in analytical centrifuge

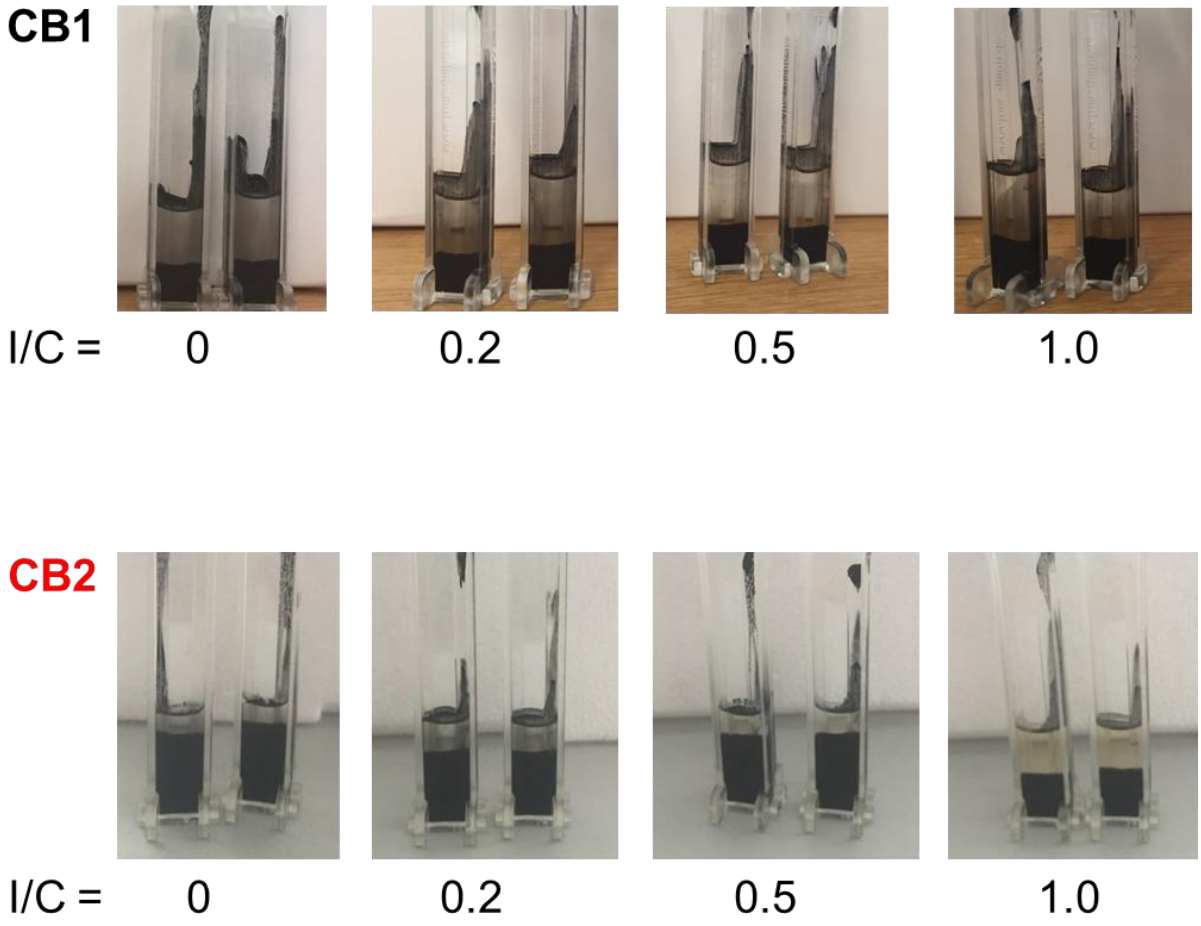

Supplementary material 13. SEM images of CB1 layers with different gap heights and *I/C* ratios

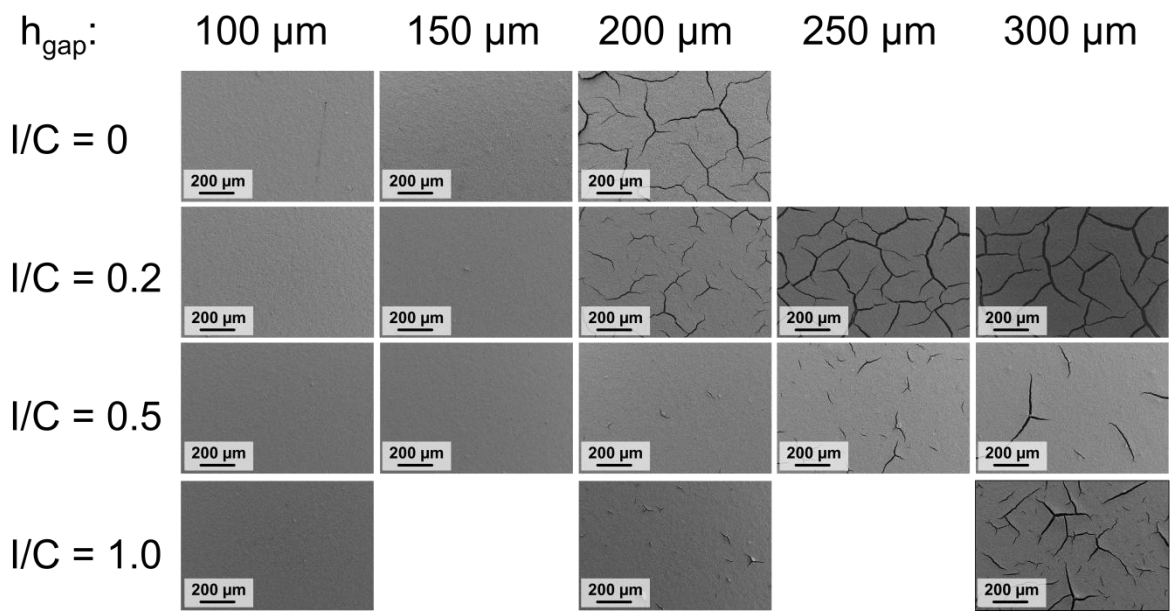

Supplementary material 14. SEM images of CB2 layers with different gap heights and *I/C* ratios

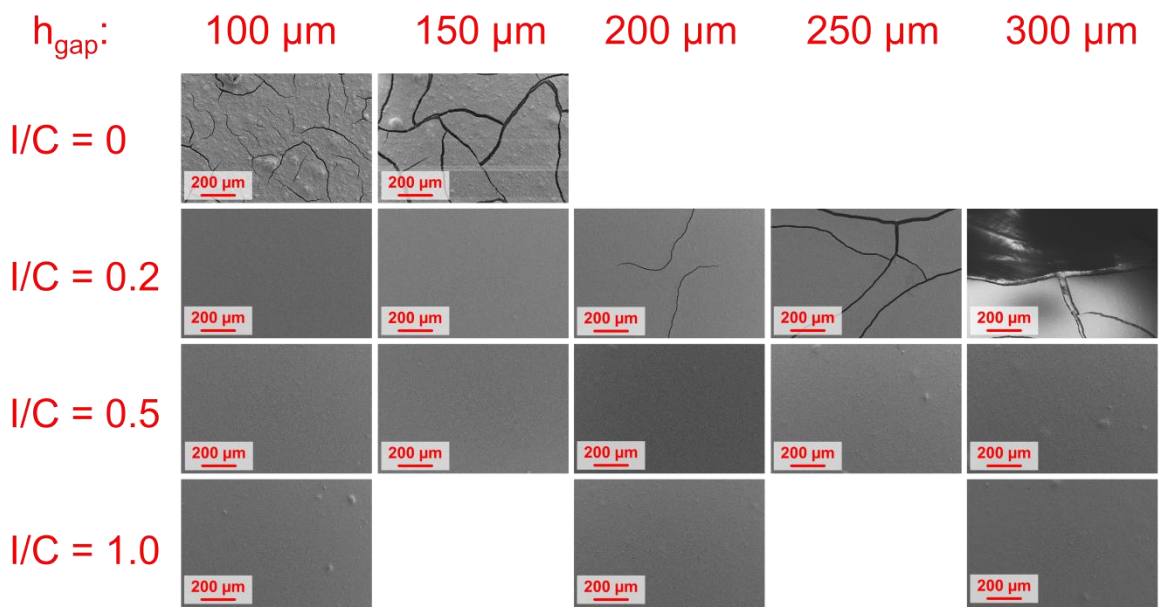

Supplementary material 15. Layer thickness (closed symbols) and layer loading (open symbols) of CB1 and CB2 layers with different *I/C* ratios formed with a gap height of 100 µm

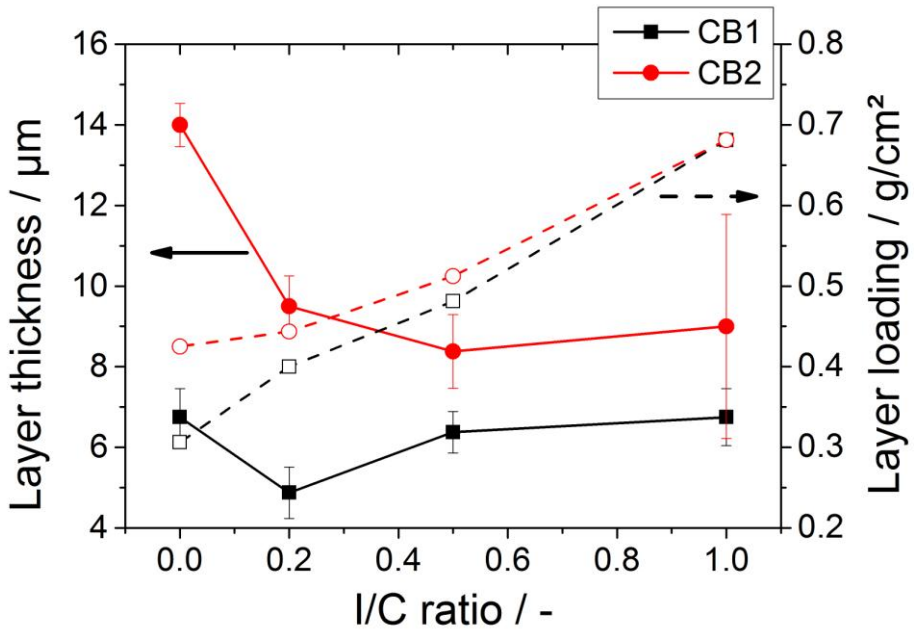

Supplementary material 16. Layer thicknesses of CB1 and CB2 layers with different *I/C* ratios depending on overall solid content (carbon black and ionomer)

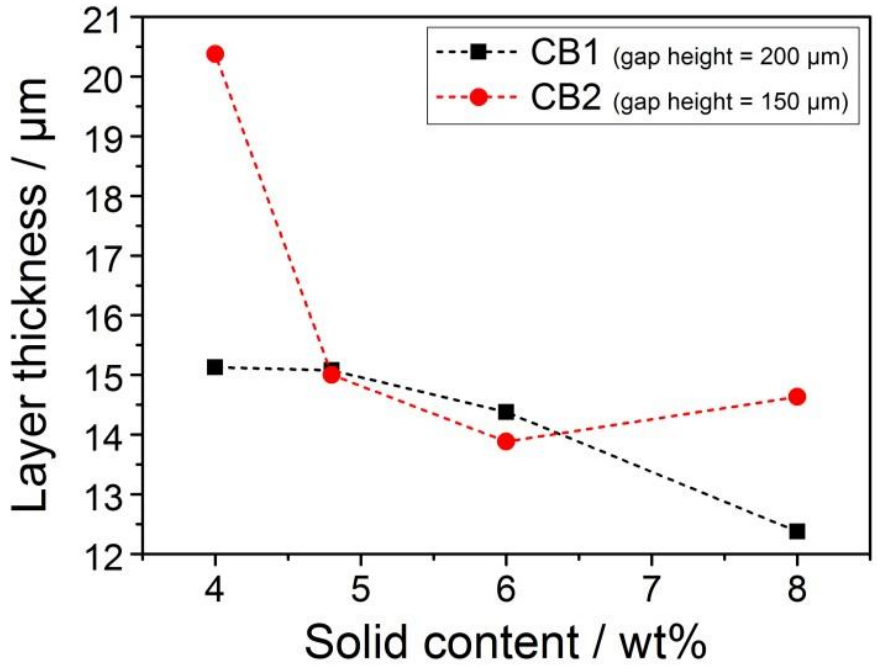

Supplementary material 17. Layer thicknesses of CB1 and CB2 layers with different *I*/*C* ratios depending on median particle size $x_{50,3}$

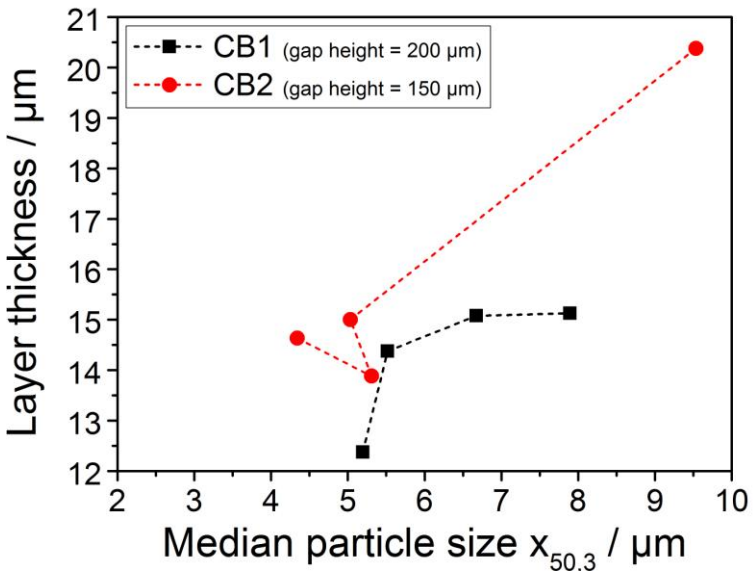

Supplementary material 18. Layer thicknesses of CB1 and CB2 layers with different *I*/*C* ratios depending on dynamic vicsosity of suspensions

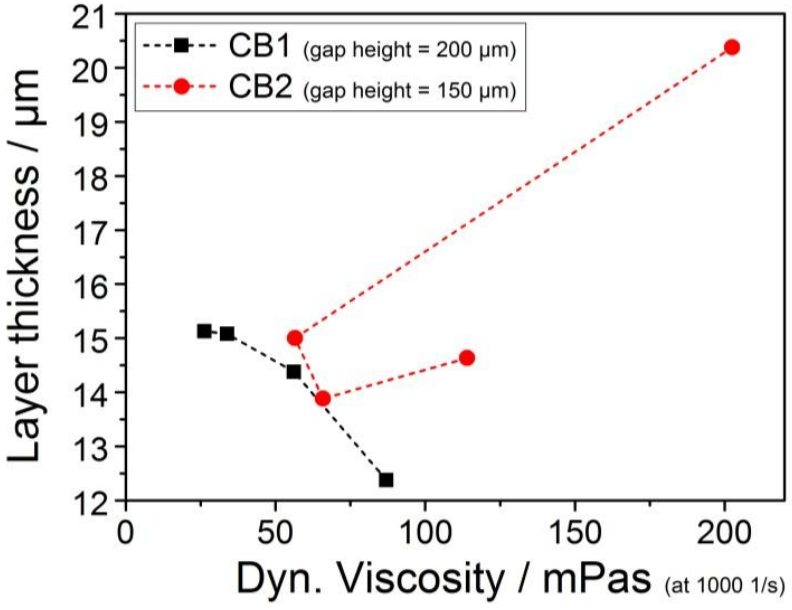

Supplementary material 19. Pore size distribution of CB1 and CB2 layers with different *I/C* ratios and pure PET-substrate determined by Hg-intrusion in high pressure region (up: density distribution, down: cumulative distribution)

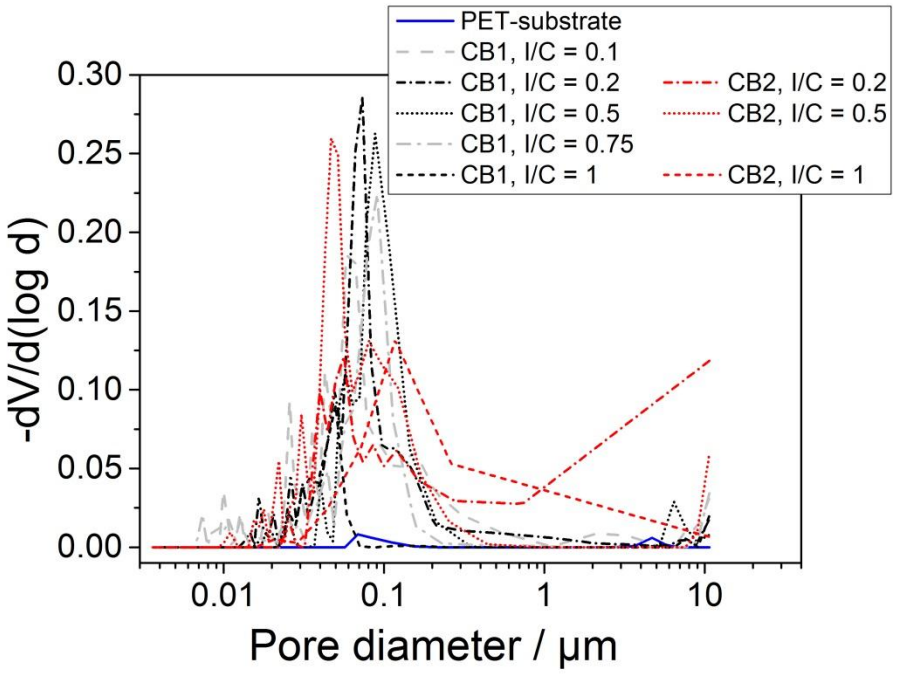

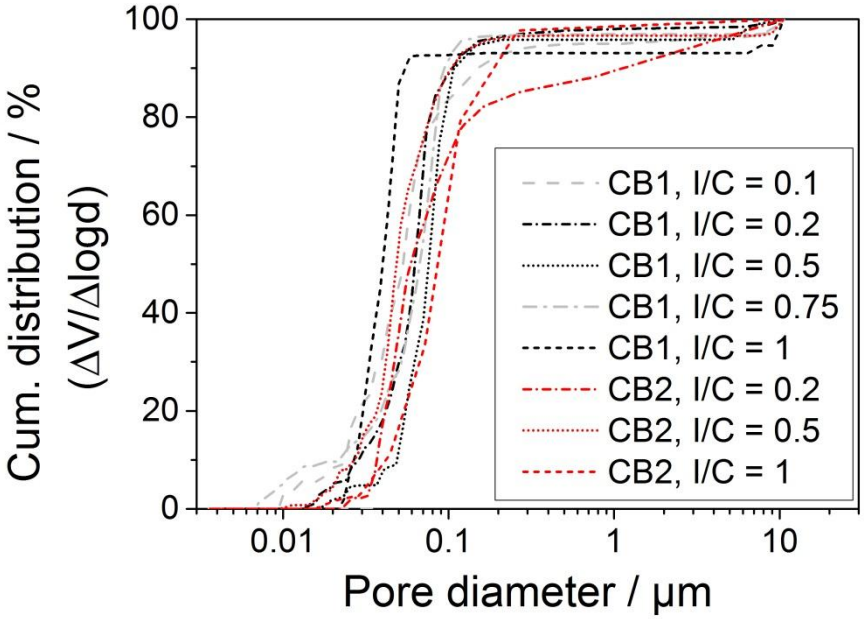

Supplementary material 20. Calculation of maximum capillary pressure for pure carbon black layers (*I*/*C* = 0) according to Singh and Tirumkudulu (2007)

$$CCT = 0.64 \left(\frac{GM\phi_{\mathrm{rcp}} r^3}{2\gamma_{\mathrm{L}}}\right)^{\frac{1}{2}} \left(\frac{2\gamma_{\mathrm{L}}}{-p_{\mathrm{cap,\,max}} r}\right)^{\frac{3}{2}}$$

→ Rewritten:

$$p_{\mathrm{cap,\,max}} = -2\gamma_{\mathrm{L}} \left[\frac{\left(\frac{GM\phi_{\mathrm{rcp}}}{2\gamma_{\mathrm{L}}}\right)^{\frac{1}{2}}}{\frac{CCT}{0.64}}\right]^{2/3}$$

Assumptions:

Shear modulus, *G* (GPa)	6.6	(mean value)*
Coordination number, *M*	6	(face centered cubic)
Liquid surface tension, γ_L (mN/m)	32.8	(87 wt% DAA in water)
Volume fraction at random close packing**, $\phi_{rcp} = 1-\varepsilon$	0.25	(for CB1)
	0.15	(for CB2)
Critical coating thickness (µm)	10.2	(for CB1)
	19.3	(for CB2)

* Shear modulus of carbon black: ca. 1.7 – 11.5 GPa (AZoNetwork UK Ltd.)

** ϕ_{rcp} is calculated by porosity ε, neglecting the fact, that the determined porosity does not only depend on the packing of the layer but also on the internal porosity of the pristine carbon black particles

→ CB1: $p_{cap,max}$ = – 551 kPa

→ CB2: $p_{cap,max}$ = – 304 kPa

Supplementary material 21. Drying curves determined with cantilever deflection method for CB1 suspension (left) and CB2 suspension (right) with *I/C* = 0 and including standard deviations

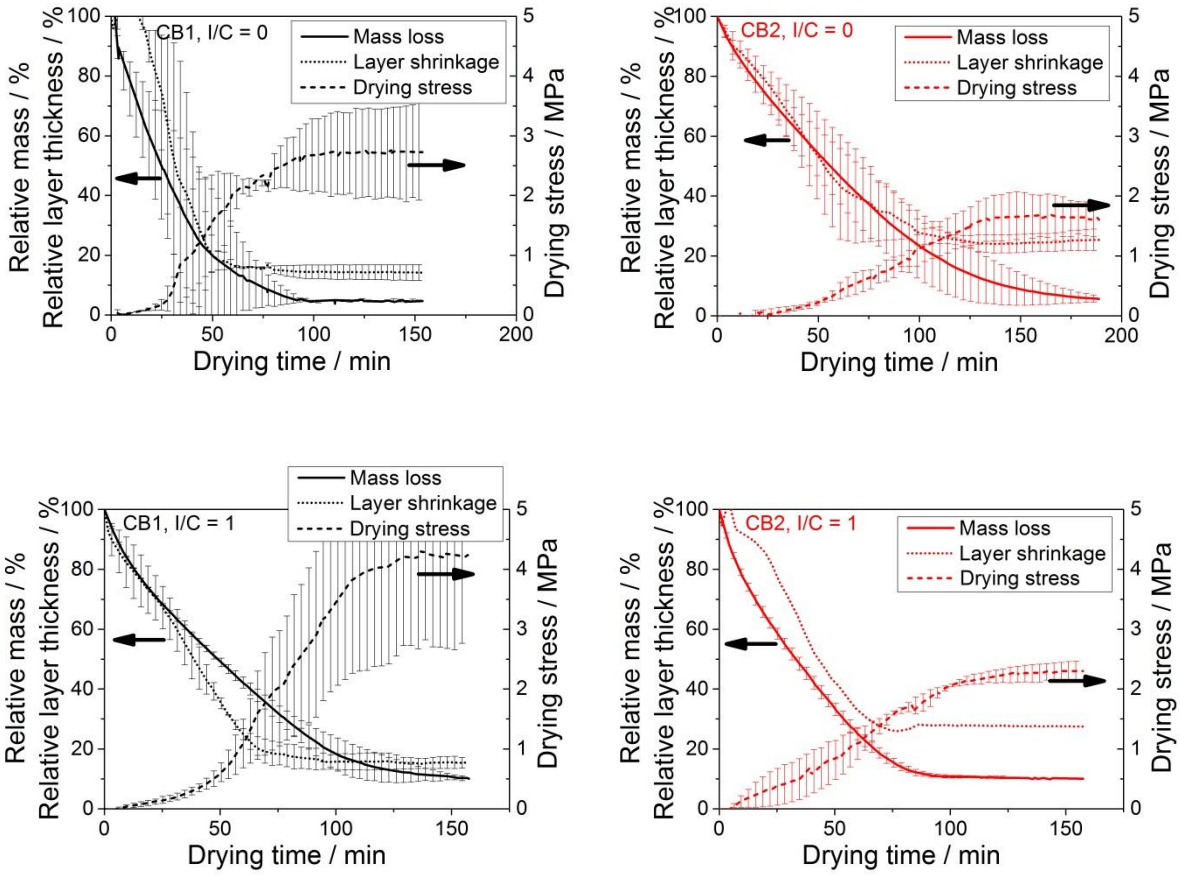

Supplementary material 22. Comparison of layer shrinkage by doctor ading and cantilever deflection on

	Relative layer thickness (%)	
	Determined by cantilever deflection method	Determined by image analysis of doctor bladed layers
CB1, $I/C = 1$	27.5	10.1
CB2, $I/C = 1$	15.4	6.6

Comparing the relative layer thicknesses, which are determined by the actual layer thickness at the end of drying divided by the gap height, layer shrinkage seems to be more pronounced for the doctor bladed layer, as the values differ by a factor of 2.4 and 2.7 respectively. However, this behavior is due to some measuring conditions. For the layer thickness, the wet layer thickness directly after the doctor blade gap is not known, but usually ca. 70% - 80% of it, depending on the menisci at the outlet of the doctor blade. Nevertheless, relative layer thickness are calculated setting the wet film thickness equal to gap height ($h_{wet} = h_{gap}$). Therefore, in reality larger relative layer thicknesses for the doctor bladed layers are assumed. Whereas the initial layer thickness prior to drying is underestimated in the doctor blade case, it is overestimated by the cantilever deflection method. After preparing the layer on the cantilever, it takes a few seconds until the cantilever is transferred and properly aligned on the balance and the measurement starts. In this “delay time” (approx. 30 s), evaporation of the solvent already starts and the initial wet film thickness at the beginning of the experiment is lower leading to larger relative layer thickness at the end of the drying run.

Supplementary material 23. Roughness (RMS) of CB1 and CB2 layers with varying ionomer content formed at a gap height of 100 µm

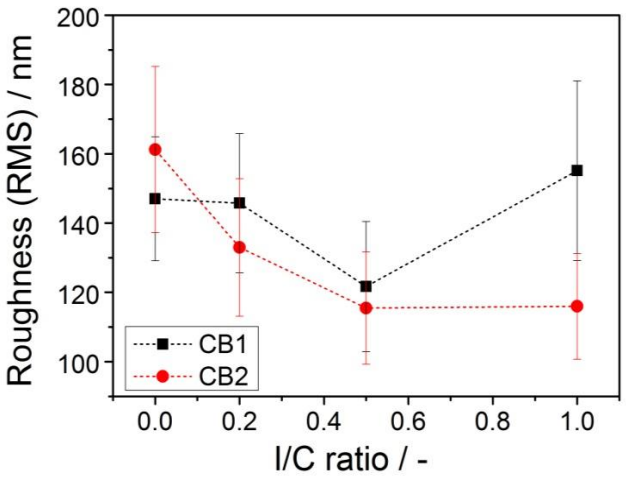

Root mean square roughness R_{RMS} was determined by AFM (Digital Instruments Nanoscope 3, tapping mode). The figure depicts R_{RMS} of the CB1 and CB2 layers with varying ionomer content. Even though standard deviations are quite large, we suppose that the general trend holds. Without ionomer CB2 forms rougher layers than CB1, as CB2 aggregates are larger.

With addition of ionomer the roughness decreases steadily for CB2, as smaller carbon black agglomerates are gained owing the stabilization effect of the ionomer. A decrease in roughness is also observed for the CB1 layers with increasing ionomer content, but above an *I*/*C* of 0.5 roughness increases again significantly. Even though this behavior is not completely understood yet, it correlates with the findings for the cracking degree. Here also an increase of the cracking was observed for *I*/*C* values larger than 0.5, even though the particle size does not change.